Revealing the Photophysics of Gold-Nanobeacons via Time-Resolved Fluorescence Spectroscopy

GUOKE WEI,[1,2] DORIN SIMIONESIE,[3] JAN SEFCIK,[3] JENS U. SUTTER,[2] QINGJIANG XUE,[2] JUN YU,[4] JINLIANG WANG,[1] DAVID J. S. BIRCH,[2] AND YU CHEN[2*]

[1]*Department of Physics, Beihang University, Beijing 100191, China*
[2]*Photophysics Group, Department of Physics, SUPA, University of Strathclyde, 107 Rottenrow, Glasgow G4 0NG, UK*
[3]*Department of Chemical and Process Engineering, University of Strathclyde, 75 Montrose Street, Glasgow G1 1XJ, UK*
[4]*Strathclyde Institute of Pharmacy and Biomedical Sciences, 204 George Street, Glasgow G1 1XW, UK*
**Corresponding author: y.chen@strath.ac.uk*

Received XX Month XXXX; revised XX Month, XXXX; accepted XX Month XXXX; posted XX Month XXXX (Doc. ID XXXXX); published XX Month XXXX

We demonstrate that time-resolved fluorescence spectroscopy is a powerful tool to investigate the conformation states of hairpin DNA on the surface of gold nanoparticles (AuNPs) and energy transfer processes in Au-nanobeacons. Long-range fluorescence quenching of Cy5 by AuNPs has been found to be in good agreement with electrodynamics modelling. Moreover, time-correlated single-photon counting (TCSPC) is shown to be promising for real-time monitoring of the hybridization kinetics of Au-nanobeacons, with up to 60% increase in decay time component and 300% increase in component fluorescence fraction observed. Our results also indicate the importance of the stem and spacer designs for the performance of Au-nanobeacons.

Energy transfer between fluorophores and gold nanoparticles (AuNPs) provides a new paradigm with which to develop novel probes for bioassays.[1,2] This is attributed to the unique physicochemical and biological properties of AuNPs, including tunable localized surface plasmon resonance (LSPR), facile surface modification, superior quenching capability, and good biocompatibility.[3-11] Among the AuNP-based nanoprobes, of particular interest is the nanobeacon that comprises a AuNP and stem-loop (hairpin) oligonucleotides dually labeled with a fluorophore at one end and a thiol moiety at the other end.[12,13] The potential advantage of the nanobeacon is that the fluorophore is still anchored to the AuNPs rather than being released into the cytoplasm upon hybridization. This makes it possible to acquire the spatial-temporal information about nucleic acid targets in living cells, offering great opportunities to understand the fundamental metabolism of cells.[14,15]

So far reports on the Au-nanobeacons have been mainly focused on steady-state fluorescence measurements.[12,13,16,17] Fluorescence lifetimes are highly sensitive to the presence of energy transfer processes, which can provide invaluable information that is unavailable from steady-state fluorescence spectroscopy.[18] In this letter, we took a novel aspect from time-resolved fluorescence spectroscopy to gain further insight into the sensing performance and energy transfer processes of Au-nanobeacons. Moreover, we demonstrated that TCSPC measurement could be used as a powerful tool to reveal the time evolutions of both fluorescence intensity and lifetime during the hybridization processes. The results also show important pointers to nanobeacon design in order to optimize their sensing performance.

The 13 nm AuNPs were synthesized by the sodium citrate reduction method.[19] Three types of Cy5-labeled hairpin DNAs (Cy5-hpDNAs), which have the same loop sequence, but different stems and spacers (Table 1), were assembled on AuNPs through a salt-aging process.[20] Note that hpCy5f consists of a five-nucleotide (5-nt) overhang at the 5' end. The nanobeacons were purified by seven successive rounds of centrifugation (13,300 rpm, 15 min, 4 °C) using 10 mM phosphate buffer (pH 7.5). The concentrations of nanobeacons were determined by UV-vis spectrophotometry (λ_{max} = 524 nm, $\varepsilon = 2.7 \times 10^8$ L·mol^{-1}·cm^{-1}).

Table 1. DNA sequences used in this work.

Name	Sequence (5' to 3')[a]	Hairpin ΔG (kcal/mol)[b]
AAhpCy5	Cy5-CTGACTTG GTG AAG CTA ACG TTG AG CAAGTCAG AA-SH	-6.84
hpCy5	Cy5-CCGGTG GTG AAG CTA ACG TTG AG CACCGG TTT TT-SH	-5.85
hpCy5f	Cy5-AA TTT AAATTGAACTTG GTG AAG CTA ACG TTG AG CAAGTTCAATTT TTT TTT TTT T-SH	-10.54
cDNA[c]	CTC AAC GTT AGC TTC AC	

[a] The underlined bases represent the stem sequence.
[b] Free energy predicted at 25 °C in 137 mM [Na^+] buffer by the UNAFold software (www. idtdna.com).
[c] Perfectly matched complementary DNA to the loop sequence.

As depicted in Fig. 1 (a), the maximum optical absorption of AuNPs was shifted from 519 to 524 nm after conjugated with hpDNAs, due to the change in the surrounding refractive index. Additionally, there is an

absorption shoulder at around 649 nm in all three nanobeacons corresponding to the absorption of Cy5, further confirming the presence of Cy5-hpDNAs on AuNPs. The surface loadings of hpDNA on AuNPs were quantitated to be 27 ± 6, 29 ± 3 and 19 ± 2 per nanoparticle for AuNP-AAhpCy5, AuNP-hpCy5 and AuNP-hpCy5f, respectively, according to a thiol exchange protocol.[21]

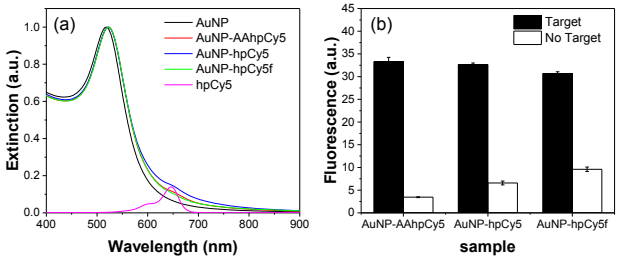

Fig. 1. (a) UV-vis spectra of "as-prepared" AuNPs, Au-nanobeacons and free hpCy5 in water. (b) Fluorescence intensity of Au-nanobeacons (1 nM) with different stems and spacers in the presence and absence of an excess of target strands (500 nM) in phosphate buffered saline (PBS) (10 mM phosphate, 137 mM NaCl, 2.7 mM KCl, pH7.4). Excitation: 635 nm; Emission: 665 nm. Error bars are one standard deviation of five measurements.

The background fluorescence (i.e., without adding cDNA) of the nanobeacons showed an increasing trend in the following order: AuNP-AAhpCy5 < AuNP-hpCy5 < AuNP-hpCy5f (Fig. 1 (b)), in line with the increasing spacer lengths used in the DNA designs (Table 1). Notably, all three nanobeacons experienced significant fluorescence recovery upon hybridization, showing comparable fluorescence intensities. This is not surprising for AuNP-AAhpCy5 and AuNP-hpCy5, as they have comparable surface coverage of hpDNAs and similar fully-extended DNA lengths (35 nt for AAhpCy5 and 34 nt for hpCy5). For AuNP-hpCy5f, the situation is more complicated since it has the lowest surface loading of hpDNA but the longest length of oligonucleotide (i.e., 56 nt).

To gain further insight into the conformational change of hpDNA on AuNPs upon hybridization, and the fluorescence quenching effect of AuNPs, we performed time-resolved fluorescence measurements on all three nanobeacons using the TCSPC technique on a FluoroCube fluorescence lifetime system (Horiba Jobin Yvon IBH Ltd., Glasgow, UK). The system was equipped with an emission monochromator and a pulsed light-emitting diode (LED) of 638 nm operating at 1 MHz repetition rate as the excitation source. The fluorescence of Cy5 was detected at 680 nm with a 32-nm slit and a 670-nm longpass filter. Fluorescence decays were measured at a magic angle (54.7°) to eliminate polarization artifacts. The acquired data are shown in Figs. 2 (a), (c) and (e).

The fluorescence intensity decay curves were initially fitted to a multiexponential model [9] using non-linear least-squares analysis:

$$I(t) = \sum_i \alpha_i \exp\left(-\frac{t}{\tau_i}\right), \quad (1)$$

where τ_i are the decay times with amplitudes α_i and $\sum \alpha_i = 1$. The fractional contribution of each lifetime component to the steady-state intensity is represented by

$$f_i = \alpha_i \tau_i \Big/ \sum_k \alpha_k \tau_k \,. \quad (2)$$

The average lifetime ($\bar{\tau}$) is calculated as

$$\bar{\tau} = \sum_i f_i \tau_i \,. \quad (3)$$

The retrieved lifetimes are summarized in Table 2.

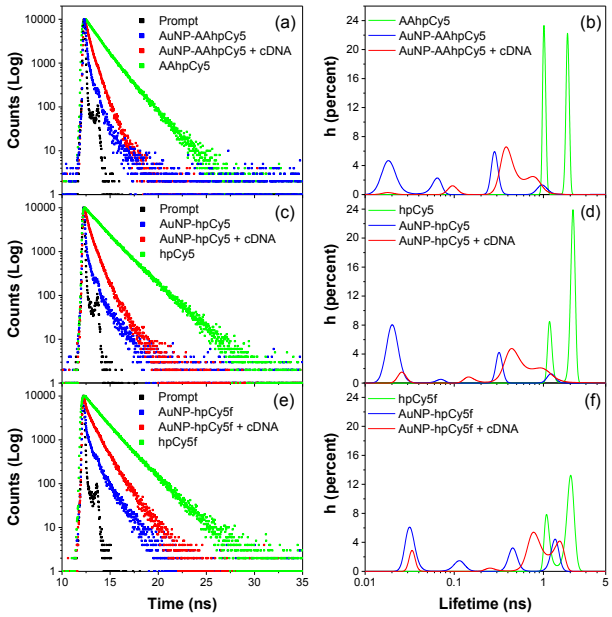

Fig. 2. (Left panel) Fluorescence intensity decay curves of (a) AuNP-AAhpCy5, (c) AuNP-hpCy5, and (e) AuNP-hpCy5f (1 nM in PBS) before and after hybridization to cDNA (500 nM). (Right panel) Fluorescence lifetime distributions of (b) AuNP-AAhpCy5, (d) AuNP-hpCy5, and (f) AuNP-hpCy5f before and after hybridization retrieved from MEM analysis. The results of corresponding free Cy5-hpDNAs are also shown in each case.

Despite small difference in the decay times of free Cy5-hpDNA in different designs, substantial reductions of lifetime are observed in all cases after Cy5-hpDNAs grafted on AuNPs, suggesting significant energy transfer from Cy5 to AuNPs. Moreover, the average lifetime of AuNP-hpCy5f in the absence of the target strands is significantly greater than those of AuNP-hpCy5 and AuNP-AAhpCy5. A short lifetime component (τ_3, <100 ps) is found in all three nanobeacons, which contributes a fraction of ~70% to the steady-state emission before hybridization, but progressively decreases after hybridization. Control experiments, using citrate-stabilized AuNPs and Cy5-free AuNP-hpDNA of same concentrations, showed no detectable signals. Therefore, the picosecond lifetime components must originate from Cy5 in a quenched state.

Upon hybridization, the fractional contributions of intermediate (τ_2) and long (τ_1) lifetime components significantly increase. It is striking to note that τ_2 is shifted to a greater value, whereas τ_1 and τ_3 remained almost constant within the uncertainty. The presence of τ_3 in the hybridized nanobeacons implies that there are still unhybridized hpDNAs on AuNPs. The presence of τ_1 in the "as-prepared" nanobeacons suggests a small amount of unfolded or improperly folded hpDNAs on AuNPs.[22,23] This should be excluded in order to quantitatively examine the influence of spacer design on the fluorescence background of the "as-prepared" nanobeacons. The background intensity in Fig. 1 (b) can thus be corrected to be 3.14, 6.04 and 7.78 (a.u.) for AuNP-AAhpCy5, -hpCy5 and -hpCy5f, respectively. Taking the surface coverage into account, it is apparent that the background fluorescence increases with increasing spacer length.

Table 2. Multiexponential analysis of fluorescence intensity decays

Sample	$\bar{\tau}$ /ns	τ_1 /ns[a]	τ_2 /ns[a]	τ_3 /ns[a]	f_1	f_2	f_3	χ_R^2
AAhpCy5	1.436	1.793 ± 0.025	0.923 ± 0.056		0.590	0.410		1.056
AuNP-AAhpCy5	0.160	0.887 ± 0.087	0.251 ± 0.031	0.032 ± 0.008	0.091	0.229	0.680	1.558
AuNP-AAhpCy5 + cDNA	0.485	0.886 ± 0.044	0.401 ± 0.030	0.092 ± 0.043	0.243	0.648	0.109	1.165
hpCy5	1.858	2.116 ± 0.022	1.110 ± 0.102		0.744	0.256		1.091
AuNP-hpCy5	0.178	1.381 ± 0.106	0.302 ± 0.038	0.027 ± 0.005	0.083	0.141	0.776	1.275
AuNP-hpCy5 + cDNA	0.521	1.017 ± 0.038	0.412 ± 0.030	0.063 ± 0.024	0.276	0.558	0.166	1.265
hpCy5f	1.718	1.990 ± 0.022	1.053 ± 0.089		0.710	0.290		1.037
AuNP-hpCy5f	0.329	1.291 ± 0.060	0.372 ± 0.051	0.037 ± 0.005	0.190	0.163	0.647	1.350
AuNP-hpCy5f + cDNA	0.800	1.300 ± 0.029	0.569 ± 0.060	0.047 ± 0.010	0.467	0.322	0.211	1.235

[a] The retrieved lifetimes are presented with three standard deviations as error.

To reveal more information on the states of Cy5 in the nanobeacons, the fluorescence decays were reanalyzed using the maximum entropy method (MEM) (Pulse 5 software, MaxEnt Ltd, Cambridge, UK).[24] This generates a lifetime distribution without any *a priori* assumptions about the decay function. The lifetime distribution $h(\tau)$ is related to the fluorescence intensity decay $I(t)$ by

$$I(t) = \int_0^\infty h(\tau) \exp\left(-\frac{t}{\tau}\right) d\tau \,. \qquad (4)$$

The recovered lifetime distributions are depicted in Figs. 2 (b), (d) and (f). Clearly, four well-separated lifetime distributions of Cy5 are found in all three nanobeacons in the absence of target strands. Upon hybridization, both of the peaks in the intermediate time range are shifted to longer lifetimes, which becomes more obvious as the spacer and the fully-extended length of oligonucleotide increase. However, no significant shifts are observed for the shortest and longest lifetime distributions. This again suggests that not all hairpins on AuNPs are hybridized and that a small amount of unfolded hpDNAs are presented in the as-prepared nanobeacons, in line with the multiexponential analysis. As noted, there is a continuous lifetime distribution consisting of two broad peaks in the long time domain in the hybridized nanobeacons. The relatively broad lifetime distributions indicate that the Cy5 molecules in the open hpDNAs are likely in a range of distances from the surface of AuNPs due to the semi-flexibility of the unpaired nucleotides at the 3' and 5' ends.

Considering the biexponential decay of free Cy5-hpDNAs and two major states (i.e., closed or open) of hpDNAs on AuNPs, it is most likely that the two lifetime components in the short time domain and the two lifetime components in the long time domain are corresponding to the closed and open Cy5-hpDNAs, respectively. Accordingly, the energy transfer efficiencies in the Cy5-AuNP systems can be determined using eqn (5):[18]

$$E = 1 - \frac{\tau_{DA}}{\tau_D} \,. \qquad (5)$$

where τ_{DA} and τ_D represent the amplitude-weighted lifetimes of Cy5 in the presence and absence of AuNPs, respectively. The calculated quantum efficiencies of energy transfer are plotted in Fig. 3 (a) as a function of Cy5-AuNP distance, considering the closed Cy5-hpDNAs in the as-prepared nanobeacons and the open Cy5-hpDNAs in the hybridized nanobeacons. The Cy5-AuNP separations are estimated by taking 4.3 Å per base for single-stranded DNA (ssDNA), 3.4 Å per basepair for double-stranded DNA (dsDNA), 1.5 Å for the C-C bond in the methylene linker and 2.3 Å for the Au-S bond.[25-27] In addition, the ssDNA spacers in the "as-prepared" nanobeacons are assumed to be fully stretched where the extension of ssDNA is the contour length, while the ssDNA fragments in the hybridized hairpins are considered as semi-flexible chains whose length is approximately twice the radius of gyration.[25,28] The radius of gyration is given as the square root of one-third of the product of contour length and persistence length (10.5 Å for ssDNA in PBS).[25]

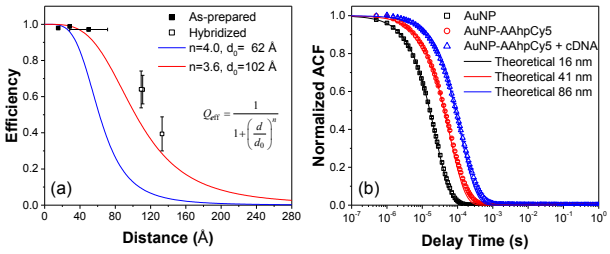

Fig. 3. (a) Energy transfer efficiency plotted versus Cy5-AuNP separations obtained from the MEM analysis and two theoretical models: an NSET model (n = 4, d_0 = 62 Å) and an electrodynamics model (n = 3.6, d_0 = 102 Å). The horizontal error bar represent the flexibility of the 5-nt overhang in the closed-state hpCy5f. Inserted is the formula of distance-dependent energy transfer efficiency. (b) Measured ACFs for AuNPs and Au-nanobeacons. Solid lines show theoretical ACFs for monodisperse populations of particles with the diameter equal to the mean hydrodynamic diameter estimated from the initial decay.

Also plotted in Fig. 3 (a) are the theoretically distance-dependent energy transfer efficiencies from Cy5 to AuNPs derived from a nanometal surface energy transfer (NSET) model[29] and an electrodynamics modeling fitting result of 10-nm AuNPs reported by Chhabra *et al.*,[30] respectively. In the NSET model, the characteristic distance length d_0 at which the energy transfer efficiency is 50% is calculated to be 62 Å, using a quantum yield of 0.2[31] and an angular frequency of 2.83×10^{15} s^{-1} for Cy5. It can be seen that the NSET model greatly underestimates the quantum efficiency of energy transfer between Cy5 and the 13-nm AuNPs, while the electrodynamics model shows a better agreement with the experiment data.

To validate these results based on beacon-intrinsic parameters with an independent measurement, we used dynamic light scattering (DLS) to measure the hydrodynamic radii of AuNPs and Au-nanobeacons.[32] As depicted in Fig. 3 (b), the shift in the measured autocorrelation functions (ACFs) shows a clear increase in the mean hydrodynamic diameter from the AuNPs to the folded AuNP-AAhpCy5 and then, in the presence of cDNA, the nanobeacons extent further increasing the mean hydrodynamic diameter. A similar behaviour was found in AuNP-hpCy5f. The DLS results are consistent with the fluorescence

spectroscopic measurement and confirmed the mechanic function of the nanobeacons.

Furthermore, TCSPC measurements were conducted to simultaneously reveal the real-time changes of both fluorescence intensity and lifetime of Cy5 in all three nanobeacons during the hybridization processes. Sequential fluorescence decays were acquired with a data-collection time of 60 s. The data was fitted to the sum of three exponentials in a batch mode, recovering time-evolution fluorescence intensity and amplitude-weighted lifetime (Fig. 4). The relative background intensity ratios are consistent with the steady-state fluorescence measurements (Fig. 1 (b)). Significantly, all three nanobeacons responded to the addition of cDNA immediately, showing an increasing fluorescence intensity and amplitude-weighted lifetime. This again confirms the conformational switching of the hpDNAs on AuNPs in the hybridization events. Moreover, it reveals that the time evolution of the amplitude-weighted lifetime matches well with the fluorescence intensity. Interestingly, AuNP-hpCy5 showed the most rapid fluorescence response to cDNA addition, while AuNP-hpCy5f exhibited the slowest fluorescence recovery rate. This is attributed to the different stems used in the hpDNAs. As the number of basepairs in the stems increases, the free energy (ΔG) decreases (Table 1), leading to a sluggish conformational switching. This suggests the importance of stem design in order to realize optimal performance, consistent with previous findings on molecular beacons.[33]

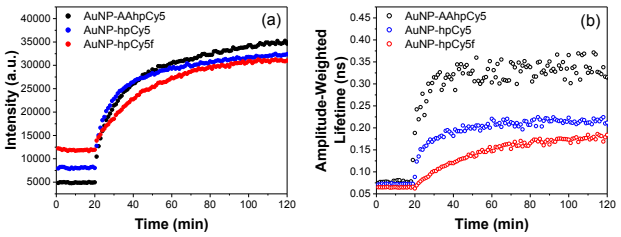

Fig. 4. TCSPC measurements of the nanobeacons upon hybridizations: (a) kinetics of fluorescence intensity; (b) kinetics of fluorescence lifetime. For each measurement, two steps were distinguished : (1) the cuvette was filled with 1 nM nanobeacons dispersed in PBS; (2) an excess of cDNA (final concentration of 500 nM) was added. The transition took place immediately after adding cDNA at the time of 20 min.

In summary, we have demonstrated that time-resolved fluorescence spectroscopy is a versatile tool to investigate conformational switching and energy transfer processes of Au-nanobeacons. The long-range fluorescence quenching of Cy5 by AuNPs has been revealed, showing good agreement with electrodynamics modelling. TCSPC has been shown to be promising for real-time monitoring of hybridization events using Au-nanobeacons.

Acknowledgements

The authors acknowledge P. Yip, P. Gu, and W. Li for assistance in experimental work. This work was supported by a BBSRC Award (BB/K013416/1). G. Wei acknowledges financial support from China Scholarship Council (CSC).

References

1. Ray, P.C.; Fan, Z.; Crouch, R.A.; Sinha, S.S.; Pramanik, A. *Chem. Soc. Rev.* **2014**, 43, 6370.
2. Zhang, Y.; Wei, G.; Ju, Y.; Birch, D. J. S.; Chen, Y. *Faraday Discuss*. **2014,** 178, 383-394.
3. Zhang, Y.; Birch, D.J.S.; Chen, Y. *Appl. Phys. Lett.* **2011,** 99, 103701.
4. Chen, Y.; Preece J.A.; Palmer, R. E. *Ann. N. Y. Acad. Sci.* **2008,** 1130, 201.
5. Zhang, Y.; Yu, J.; Birch, D.J.S.; Chen, Y. *J. Biomed. Opt*. **2010,** 15, 020504-3.
6. Gu, P.; Birch, D.J.S.; Chen, Y. *Methods Appl. Fluoresc.* **2014,** 2, 024004.
7. Rachnor, C.; Singh, M. R.; Zhang, Y.; Birch, D.J.S.; Chen, Y. *Methods Appl. Fluoresc*. **2014,** 2, 015002.
8. Chen, Y.; Zhang, Y.; Birch, D.J.S.; Barnard, A.S. *Nanoscale* **2012,** 4, 5017.
9. Li, D.D.; Yu, H.; Chen, Y. *Opt. Lett*., **2015,** 40, 336.
10. Zhang, Y.; Xu, D.; Li, W.; Yu, J.; Chen, Y. *J. Nanomater*., **2012**, 375496 - 7. doi:10.1155/2012/375496.
11. Boisselier, E.; Astruc, D. *Chem. Soc. Rev*. **2009,** 38, 1759.
12. Dubertret, B.; Calame, M.; Libchaber, A.J. *Nat. Biotechnol*. **2001,** 19, 365 .
13. Song, S.; Liang, Z.; Zhang, J.; Wang, L.; Li, G.; Fan, C. *Angew. Chem. Int. Ed*. **2009,** 48, 8670.
14. Holt, C.E.; Bullock, S.L. *Science* **2009,** 326, 1212.
15. Eliscovich, C.; Buxbaum, A.R.; Katz, Z.B; Singer, R.H. *J. Biol. Chem*. **2013,** 288, 20361.
16. Jayagopal, A.; Halfpenny, K.C.; Perez, J.W; Wright, D.W. *J. Am. Chem. Soc.* **2010,** 132, 9789.
17. Pan, W.; Zhang, T.; Yang, H.; Diao, W.; Li, N.; Tang, B. *Anal. Chem.* **2013,** 85, 10581.
18. Lakowicz, J.R. *Principles of Fluorescence Spectroscopy*, 3rd Ed (Springer, New York, 2006).
19. Grabar, K.C.; Freeman, R.G.; Hommer, M.B.; Natan, M.J. *Anal. Chem*. **1995,** 67, 735.
20. Hurst, S.J.; Lytton-Jean, A.K.R; Mirkin, C.A. *Anal. Chem.* **2006**, 78, 8313.
21. Demers, L.M.; Mirkin, C.A.; Mucic, R.C.; Reynolds, R.A.; Letsinger, R.L.; Elghanian, R.; Viswanadham, G. *Anal. Chem.* **2000,** 72, 5535.
22. Cederquist, K.B.; Golightly, R.S.; Keating, C.D. *Langmuir* **2008,** 24, 9162.
23. Bonnet, G.; Krichevsky, O.; Libchaber, A. *Proc. Natl. Acad. Sci. U. S. A*. **1998,** 95, 8602.
24. Brochon, J. *Methods Enzymo*l. **1994,** 240, 262.
25. Tinland, B.; Pluen, A.; Sturm, J.; Weill, G. *Macromolecules* **1997,** 30, 5763.
26.Peng, H.I.; Strohsahl, C.M.; Leach, K.E.; Krauss, T.D.; Miller, B.L. *ACS Nano* **2009, 3**, 2265.
27. Häkkinen, H. *Nat. Chem*. **2012,** 4, 443.
28. Parak, W.J.; Pellegrino, T.; Micheel, C.M.; Gerion, D.; Williams, S.C.; Alivisatos, A P. *Nano Lett.* **2003,** 3, 33.
29.Yun, C.S.; Javier, A.; Jennings, T.; Fisher, M.; Hira, S.; Peterson, S.; Hopkins, B.; Reich, N.O.; Strouse, G.F. *J. Am. Chem. Soc.* **2005,** 127, 3115.
30. Chhabra, R.; Sharma, J.; Wang, H.; Zou, S.; Lin, S.; Yan, H.; Lindsay, S.; Liu, Y. *Nanotechnology* **2009,** 20, 485201.
31.Malicka, J.; Gryczynski, I.; Fang, J.; Lakowicz, J.R. *Anal. Biochem*. **2003,** 317, 136.
32. Finsy, R. *Adv. Colloid Interface Sci.* **1994,** 52, 79.
33. Tsourkas, A.; Behlke, M.A.; Rose, S.D.; Bao, G. *Nucleic Acids Res.* **2003,** 31, 1319.

Full references

[1] Ray, P. C.; Fan, Z.; Crouch, R. A.; Sinha, S. S.; Pramanik, A. Nanoscopic Optical Rulers beyond the FRET Distance Limit: Fundamentals and Applications. *Chem. Soc. Rev.* **2014**, *43*, 6370–6404.

[2] Zhang, Y.; Wei, G.; Yu, J.; Birch, D. J. S.; Chen, Y. Surface plasmon enhanced energy transfer between gold nanorods and fluorophores: application to endocytosis study and RNA detection. *Faraday Discuss*. **2015**, *178*, 383-394.

[3] Zhang, Y.; Yu, J.; Birch, D. J. S.; Chen, Y. Energy transfer between DAPI and gold nanoparticles under two-photon excitation. *Appl. Phys. Lett.* **2011**, *99*, 103701

[4] Chen, Y.; Preece, J. A.; Palmer, R. E. Processing and characterization of gold nanoparticles for use in plasmon probe spectroscopy and microscopy of biosystems. *Ann. N. Y. Acad. Sci*. **2008**, *1130,* 201-206.

[5] Zhang, Y.; Yu, J.; Birch, D. J. S.; Chen, Y. Gold nanorods for applications in biological imaging. *J. Biomed. Opt.* **2010,** *15*, 020504-3.

[6] Gu, P.; Birch, D. J. S.; Chen, Y. Dye-dope polystyrene-coated gold nanorods: towards wavelength tuneable SPASER. *Methods Appl. Fluoresc*. **2014**, *2***,** 024004.

[7] Rachnor, C.; Singh, M. R.; Zhang, Y.; Birch D. J. S.; Chen, Y. Energy transfer between a biological labelling dye and gold nanorods. *Methods Appl. Fluoresc*. **2014**, *2,* 015002.

[8] Chen, Y.; Zhang, Y.; Birch, D. J. S.; Barnard, A. S. Creation and luminescence of size selected gold nanorods. *Nanoscale* **2012**, *4*, 5017-5022.

[9] Li, D. D.; Yu, H.; Chen, Y. Fast bi-exponential fluorescence lifetime imaging microscopy techniques, *Opt. Lett.*, **2015,** *40*, 336-339.

[10] Zhang, Y.; Xu, D.; Li, W.; Yu, J.; Chen, Y. Effect of Size, Shape and Surface Modification on Cytotoxicity of Gold Nanoparticles to Human HEp-2 and Canine MDCK Cells. *J. Nanomater.*, **2012**, *2012*, 375496-7. doi:10.1155/2012/375496.

[11] Boisselier, E.; Astruc, D. Gold Nanoparticles in Nanomedicine: Preparations, Imaging, Diagnostics, Therapies and Toxicity. *Chem. Soc. Rev.* **2009**, *38*, 1759–1782.

[12] Dubertret, B.; Calame, M.; Libchaber, A. J. Single-Mismatch Detection Using Gold-Quenched Fluorescent Oligonucleotides. *Nat.Biotechnol.* **2001**, *19*, 365–370.

[13] Song, S.; Liang, Z.; Zhang, J.; Wang, L.; Li, G.; Fan, C. Gold-Nanoparticle-Based Multicolor Nanobeacons for Sequence-Specific DNA Analysis. *Angew. Chemie - Int. Ed.* **2009**, *48*, 8670–8674.

[14] Holt, C. E.; Bullock, S. L. Subcellular mRNA Localization in Animal Cells and Why It Matters. *Science* **2009**, *326*, 1212–1216.

[15] Eliscovich, C.; Buxbaum, A. R.; Katz, Z. B.; Singer, R. H. mRNA on the Move: The Road to Its Biological Destiny. *J. Biol. Chem.* **2013**, *288*, 20361–20368.

[16] Jayagopal, A.; Halfpenny, K. C.; Perez, J. W.; Wright, D. W. Hairpin DNA-Functionalized Gold Colloids for the Imaging of mRNA in Live Cells. *J. Am. Chem. Soc.* **2010**, *132*, 9789–9796.

[17] Pan, W.; Zhang, T.; Yang, H.; Diao, W.; Li, N.; Tang, B. Multiplexed Detection and Imaging of Intracellular mRNAs Using a Four-Color Nanoprobe. *Anal. Chem.* **2013**, *85*, 10581–10588.

[18] Lakowicz, J. R. *Principles of Fluorescence Spectroscopy*; 3rd Ed.; Springer: New York, 2006.

[19] Grabar, K. C.; Freeman, R. G.; Hommer, M. B.; Natan, M. J. Preparation and Characterization of Au Colloid Monolayers. *Anal. Chem.* **1995**, *67*, 735–743.

[20] Hurst, S. J.; Lytton-Jean, A. K. R.; Mirkin, C. A. Maximizing DNA Loading on a Range of Gold Nanoparticle Sizes. *Anal. Chem.* **2006**, *78*, 8313–8318.

[21] Demers, L. M.; Mirkin, C. A.; Mucic, R. C.; Reynolds, R. A.; Letsinger, R. L.; Elghanian, R.; Viswanadham, G. A Fluorescence-Based Method for Determining the Surface Coverage and Hybridization Efficiency of Thiol-Capped Oligonucleotides Bound to Gold Thin Films and Nanoparticles. *Anal. Chem.* **2000**, *72*, 5535–5541.

[22] Cederquist, K. B.; Golightly, R. S.; Keating, C. D. Molecular Beacon-Metal Nanowire Interface: Effect of Probe Sequence and Surface Coverage on Sensor Performance. *Langmuir* **2008**, *24*, 9162–9171.

[23] Bonnet, G.; Krichevsky, O.; Libchaber, A. Kinetics of Conformational Fluctuations in DNA Hairpin Loops. *Proc. Natl. Acad. Sci. U. S. A.* **1998**, *95*, 8602–8606.

[24] Brochon, J. Maximum Entropy Method of Data Analysis in Time-Resolved Spectroscopy. *Methods Enzymol.* **1994**, *240*, 262–311.

[25] Tinland, B.; Pluen, A.; Sturm, J.; Weill, G. Persistence Length of Single-Stranded DNA. *Macromolecules* **1997**, *30*, 5763–5765.

[26] Peng, H. I.; Strohsahl, C. M.; Leach, K. E.; Krauss, T. D.; Miller, B. L. Label-Free DNA Detection on Nanostructured Ag Surfaces. *ACS Nano* **2009**, *3*, 2265–2273.

[27] Häkkinen, H. The Gold-Sulfur Interface at the Nanoscale. *Nat. Chem.* **2012**, *4*, 443–455.

[28] Parak, W. J.; Pellegrino, T.; Micheel, C. M.; Gerion, D.; Williams, S. C.; Alivisatos, a. P. Conformation of Oligonucleotides Attached to Gold Nanocrystals Probed by Gel Electrophoresis. *Nano Lett*. **2003**, *3*, 33–36.

[29] Yun, C. S.; Javier, A.; Jennings, T.; Fisher, M.; Hira, S.; Peterson, S.; Hopkins, B.; Reich, N. O.; Strouse, G. F. Nanometal Surface Energy Transfer in Optical Rulers, Breaking the FRET Barrier. *J. Am. Chem. Soc.* **2005**, *127*, 3115–3119.

[30] Chhabra, R.; Sharma, J.; Wang, H.; Zou, S.; Lin, S.; Yan, H.; Lindsay, S.; Liu, Y. Distance-Dependent Interactions between Gold Nanoparticles and Fluorescent Molecules with DNA as Tunable Spacers. *Nanotechnology* **2009**, *20*, 485201.

[31] Malicka, J.; Gryczynski, I.; Fang, J.; Lakowicz, J. R. Fluorescence Spectral Properties of Cyanine Dye-Labeled

DNA Oligomers on Surfaces Coated with Silver Particles. *Anal. Biochem.* **2003**, *317*, 136–146.

[32] Finsy, R. Particle Sizing by Quasi-Elastic Light Scattering. *Adv. Colloid Interface Sci.* **1994**, *52*, 79–143.

[33] Tsourkas, A.; Behlke, M. A; Rose, S. D.; Bao, G. Hybridization Kinetics and Thermodynamics of Molecular Beacons. *Nucleic Acids Res.* **2003**, *31*, 1319–1330.